14th Australasian Fluid Mechanics Conference
Adelaide University, Adelaide, Australia
10-14 December 2001

Convective Circulation Driven by a Non-uniform Bottom Heat Flux and a Localised Salinity Flux.

Julia C. Mullarney, Ross W. Griffiths and Graham O. Hughes

Research School of Earth Sciences
Australian National University, Canberra, ACT, 0200 AUSTRALIA

Abstract

The thermal convection in a basin driven by a horizontal variation of surface temperature was originally proposed by Stommel [11] and Rossby [7] as a useful, simple model of thermohaline circulation in the oceans. We return to the problem and report experiments in which we impose a uniform heat flux into a long tank over one half of its base and cool the other half, achieving large Rayleigh numbers and small aspect ratios. A stable thermocline over the cooled base flows towards the heated end, where for sufficiently large Rayleigh numbers it is eroded by a convective mixed layer that deepens towards the heated ('polar') end of the basin. We also add to the thermal convection a stabilising salinity buoyancy flux imposed at one end of the basin, mimicking a freshwater buoyancy flux into polar oceans. Large steady salt fluxes lead to a permanent layering and cessation of deep convection. For smaller salt fluxes we observe a periodic breakdown of a 'polar' halocline and an oscillation in the strength of the localised deep convection.

Introduction

The global thermohaline circulation of the oceans is driven largely by latitudinal gradients of thermal, moisture and wind stress boundary conditions at the ocean surface. With thermal forcing alone, the heat input at low latitudes and heat loss at high latitudes maintains a density gradient at the surface, driving a poleward surface flow (Stommel [11]). Downwelling convection occurs at high latitudes. There must be a compensating return flow at depth and upwelling elsewhere, possibly at low latitudes. Under present climatic conditions the deep polar convection produces the Deep and Bottom Waters of the oceans and the equatorward return flow is at great depths below the thermocline. An important point is that the location of forcing at only one boundary leads to asymmetric flow, with the downwelling deep convection being tightly confined in the polar regions.

The smallness of the sinking regions was demonstrated nicely by Rossby [7] using a laboratory model in which convection was forced by a linear temperature gradient imposed along the base of a tank. This work was followed by a numerical simulation of a similarly forced flow in a square box (Rossby, [8]). The key observations were: 1) the convection approached a steady state in which the heat content of the tank was constant; 2) a stable thermal boundary layer formed over the cooled part of the base; and 3) a narrow upwelling boundary layer on the vertical end wall above the heated end of the base carried heat to the top and ventilated the whole of the water column. Thus the highly localised nature of high-latitude deep convection in the oceans may be seen as an inevitable consequence of the basin scale gradient of thermal forcing at the surface. It is not necessary to appeal to local conditions or mechanisms, such as geography, atmospheric forcing, surface salinity or pre-conditioning of the water column, in polar oceans, although any of these factors may influence the detailed location of the deep sinking of dense waters.

Another critical factor influencing the thermohaline circulation is the distribution of boundary buoyancy fluxes due to freshwater input, precipitation and evaporation (which we refer to here as salinity buoyancy fluxes). There is an excess of evaporation at low and mid-latitudes and an inflow of relatively fresh water into polar oceans from rivers and icesheets (Broecker *et al*. [2], Rahmstorf [6]). The apparent sensitivity of deep convection regimes in the North Atlantic to the salinity in the Arctic Ocean and Norwegian Sea, as inferred from paleoclimate records (*e.g*. Bard *et al*. [1]) and ocean general circulation models (*e.g*. Wadley *et al.* [12]), has led to extensive discussion of the effects of variations in freshwater influx from icesheets associated with past and future climate variations. In particular, global ocean models have predicted the possibility of significant changes in the thermohaline circulation pattern as a consequence of variations of the fresh water fluxes resulting from atmospheric climate change (*e.g*. Thual & McWilliams [10], Manabe & Stouffer [5]), or even as a result of internal ocean dynamics with fixed boundary conditions (*e.g*. Winton & Sarachik [13], Lenderink & Haarsma [4]).

Given the complexity of the ocean circulation dynamics and the relevance of Rossby's [7] laboratory thermal convection experiment, we use a similar arrangement and add a salinity (freshwater) buoyancy flux at the 'polar' end of a basin. The introduction of a salinity buoyancy flux independent of the heat flux adds enormous complexity to the flow behaviour and leads to time-dependent solutions for steady boundary conditions. We have also increased the length of the laboratory tank by a factor of five (and the volume by a factor of 20) over that used by Rossby [7, 8] in order to increase the Rayleigh number, decrease the aspect ratio and reduce sidewall heat losses. In addition we have modified the fixed-temperature boundary conditions in favour of an imposed heat flux.

The Convection tank

We use a tank of length L = 1.2m long, width W = 150mm and select a water depth D = 200mm for all experiments (figure 1). The first series of these experiments were carried out in a pre-existing tank with 6mm glass walls. These were insulated with 100mm of expanded polystyrene foam on the ends and on the water surface, and by removable sheets of 50mm foam on the two side walls. The base of the tank was a single plate of 6mm aluminium. The right hand half of the base sat on a heat exchanger consisting of an aluminium block containing channels for coolant recirculation capped by a 10mm-thick copper plate. The left half of the base sat on an electric heating mat which was designed to provide a uniform power dissipation F_T (Wm^{-2}) over its 600mm x 150mm area, giving a *total* heat flux $F_T WL/2$.

The flux boundary condition implies that in reaching a steady state the boundary temperature at the cooled end of the tank must adjust until the conductive flux integrated over the area of the cold plate matches the imposed heat input at the heated end. We chose to use the fixed-flux boundary condition at the heated end for its convenience in scaling of the flow. Furthermore, the flux condition is relevant given the

predominance of radiative heating of the ocean surface at low and mid-latitudes. The piece-wise uniform heating of the boundary was chosen for ease of production, since a linear gradient of temperature or heat flux is relatively difficult to achieve over distances of order 1m. Numerical simulations of purely thermal convection in a square box with bottom temperature distributions differing from a linear gradient (Rossby [8]) predict a larger heat flux for the same overall temperature difference ΔT when the gradient is more tightly confined to the centre of the base. However, the fundamental features and behaviour of the flow are similar.

A second tank of the same dimensions but with improved insulation and heat exchangers is under construction. Additional experiments are also planned with the heating mat replaced with a second recirculating heat exchanger fed from a controlled hot water bath.

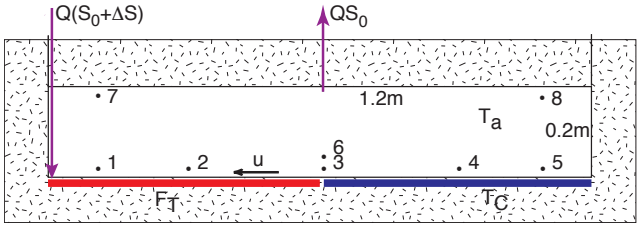

Figure 1. Sketch of the convection tank showing thermistor locations. The horizontal locations of thermistors shown were x = 0.1, 0.3, 0.6, 0.9 and 1.1m (x = 0 the left end of the tank). When they were held stationary to obtain time records, thermistors were at z = 10mm (#1 - 5), z = 30mm (#6) and at z = 170mm (#7, 8) above the base.

Temperature measurements were taken with eight fast-response thermistors attached to vertical shafts so that they could readily be relocated to any depth or traversed to obtain vertical profiles (figure 1). In order to minimise variations with temperature of the thermal expansion coefficient α, a 10% salt solution was used as the working fluid and cold plate temperatures less than 5°C were avoided. Differences in α then varied, about an average value of $3.9\text{x}10^{-4}\text{K}^{-1}$, by less than 30% for temperatures between 10°C and 40°C (Ruddick & Shirtcliffe [9]). Experiments were carried out with the cold bath temperature at 0°C and the power supply to the heating mat set to $F_T WL/2$ = 137W. In the equilibrium state the tank temperature (outside the boundary layer) was $T_a \approx$ 36 - 37°C and the Rayleigh number (evaluated for fluid properties at T_a) was $Ra_F \sim 1.8\text{x}10^{13}$.

A stabilising salinity buoyancy flux was supplied as a salt solution having a concentration ΔS and density anomaly $\Delta\rho = \rho_0\beta\Delta S$ above the initial salinity S_0 and density ρ_0 of the water in the tank, where β is the salinity expansion coefficient. The salt solution was injected from a narrow horizontal slot placed across the width of the tank at the bottom left hand corner, and pumped at a constant flow rate Q (m^3s^{-1}) by a peristaltic pump. The same pump drive was fitted with a second identical head which pumped an equal flux of water out of the tank from a small tube placed either at centre top or in the bottom right hand corner. This withdrawal of water maintained a constant water volume in the tank and is considered to have no influence on the flow other than in controlling the volume of any stable bottom layer.

Scaling analysis

Non-dimensionalisation of the momentum, continuity, heat and salt equations, and a scaling of horizontal distance by L, vertical distance by D, salinity differences by ΔS, temperature differences by $\Delta T = F_T L/(\rho_0 c_p \kappa_T)$ and time by L^2/κ_T lead to the set of governing dimensionless parameters:

$$Ra_F = g\alpha F_T L^4/(\rho_o c_p \kappa_T^2 \nu),\ Pr = \nu/\kappa_T,\ A = D/L, \qquad (1)$$

$$R_\rho = \beta\Delta S/\alpha\Delta T,\ \tau = \kappa_S/\kappa_T, \qquad (2)$$

where c_p is the specific heat and the density is assumed linear:

$$\rho = \rho_0\{1 - \alpha(T - T_0) + \beta(S - S_0)\}. \qquad (3)$$

These are the flux Rayleigh number, Prandtl number, basin aspect ratio, stability ratio, and ratio of S and T diffusivities, respectively. The first three parameters (1) are common to the case of purely thermal convection. The stability ratio R_ρ compares the *input* salinity density anomaly to that due to the temperature scale ΔT and is identical to the ratio of salinity and thermal Rayleigh numbers Ra_S / Ra_F, where $Ra_S = g\beta\Delta SL^3/(\kappa_T\nu)$. The volume flux of the salinity source does not enter from the governing equations but will enter through the boundary conditions. The buoyancy flux due to the salinity source is $B_S = g\rho_0\beta\Delta SQ$ (N s^{-1}) and that due to the total heat flux is $B_T = g\alpha F_T LW/2c_p$. Hence we can write the stability ratio (which is independent of Q) as

$$R_\rho = (B_S / B_T)\, Pe^{-1}, \qquad (4)$$

where $B_S/B_T = 2\rho_0 c_p\beta\Delta SQ/(\alpha F_T LW)$ is the ratio of buoyancy fluxes and $Pe = 2QD/(\kappa_T LW)$ is a Peclet number.

Above the cooled half of the base the flow is dominated by a slow downwelling at velocity w opposing vertical conduction of heat through a stable stratification in a bottom boundary layer of depth h. For the steady state thermal convection the heat equation implies a balance between vertical advection and conduction expressed by $u \sim wL/h \sim \kappa_T L/h^2$. A balance of viscous stresses and buoyancy in the horizontal boundary layer flow implies $g\alpha\delta T(h/L) \sim \nu u/h^2$, where δT is the temperature difference across the cold boundary layer as well as the horizontal temperature difference within the boundary layer between the ends of the box. Conservation of heat also requires the integral constraint $\rho_0 c_p \delta T u h \sim F_T L$. These three relations can be solved for u, h and δT to find

$$\delta T/\Delta T \sim Ra_F^{-1/6}, \qquad (5)$$

$$h/L \sim Ra_F^{-1/6}, \qquad (6)$$

$$uL/\kappa_T \sim Ra_F^{1/3} \qquad (7)$$

and the Nusselt number

$$Nu = F_T L/(\rho_0 c_p \kappa_T \delta T) \sim Ra_F^{1/6}. \qquad (8)$$

The corresponding scaling for the case of an imposed temperature difference δT in place of the heat flux is given by Rossby [7] and has been compared with finite-element simulations of thermal convection in a square box (A = 1) with various bottom temperature distributions (Rossby [8]).

Results for thermal convection

The thermal convection itself is sensitive to initial and boundary conditions. Hence care was taken to ensure that the convection had approached its thermal equilibrium state, and that convection at the heated end penetrated through the full-depth of the box, before measurements were taken and before the salt flux was turned on.

We discovered that the thermal convection involved an unstable convective boundary layer, or mixed layer, within the otherwise stable, bottom thermal boundary layer over the heated half of the base. The heating leads to overturn of a lower portion of the cold boundary layer as it flows toward

the hot end of the box. The unstable portion deepens with distance along the base until it becomes a narrow vertical plume extending through the depth of the box against the end wall. We refer to this unstable layer as the convective mixed layer (CML). It was visible on a shadowgraph screen, in the mixing of $KMnO_4$ crystals dropped onto the base, and in synthetic schlieren images [3]. Because such an embedded unstable layer is an unusual feature of convection, brought about by the combined vertical and horizontal forcing gradients in our case, we present a simple mixed-layer model which predicts the observed CML depth.

Continuity of temperature and density at the top of the CML at $z = \eta$ require

$$d\eta/dx = (dT_m/dx) / [dT'(\eta)/dz], \quad (9)$$

where T_m is the temperature of the CML, u is the horizontal velocity (assumed uniform in the boundary layer) and $T'(z)$ is the oncoming temperature profile at $x = L/2$. Conservation of heat, neglecting conductive heat transfer into the CML from the overlying stable region, implies

$$\eta u\, dT_m/dx = F_T/\rho_0 c_p. \quad (10)$$

A model temperature profile through the stable cold boundary layer can be found by balancing vertical advection and diffusion in the presence of a uniform vertical velocity w:

$$T'(z) \approx T_a - \delta T\, e^{-z/h}, \quad (11)$$

where $\delta T = T_a - T_c$ (T_c and T_a the cold boundary and upper tank temperatures, respectively) and $h = \kappa_T/w$ is the depth of the stable boundary layer, as before. Solving (9, 10, 11) with $\eta = 0$ at $x = x^*$ ($\leq L/2$) and making use of the previous scales (5, 6, 7) for δT, h and u gives

$$k(x^* - x)/L \approx 1 - [1 + \eta/h]e^{-\eta/h}, \quad (12)$$

where k is a constant of order one. By further requiring $\eta = D$ at ($x=0$) we find the solution $\eta(x)$ for a given h (or Ra_F) and evaluate k. The solution shown in figure 2 is for h = 6mm, as appropriate for $Ra_F \sim 10^{13}$.

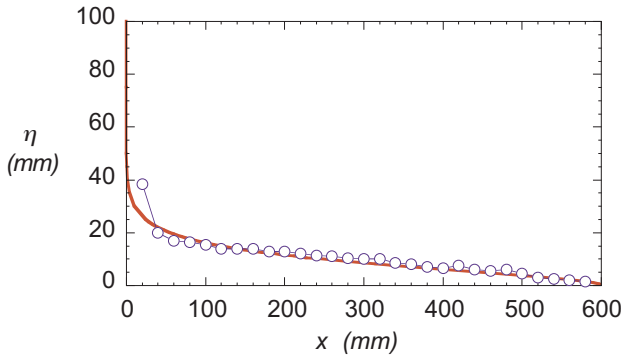

Figure 2. The depth η of the unstable convective boundary layer over the heated half of the base for thermal forcing alone: — mixed layer model; –o– measured depth. (The ordinate covers half of the depth D.)

The predicted variation of the CML depth compares well with measured depths (figure 2). The rate of CML deepening decreases with distance from its origin near $x = L/2$ because the basal heat flux is mixed into a deepening layer. However, the rate of deepening with x increases again closer to the end wall, where the CML is encroaching into a much smaller overlying density gradient. The end wall boundary layer is not included in this calculation. Hence the deep convection is confined to an infinitely thin region. However, the approach to the deep convection region is described well by the simple model. An image of the convection, obtained by the synthetic schlieren technique [3], is shown in figure 3.

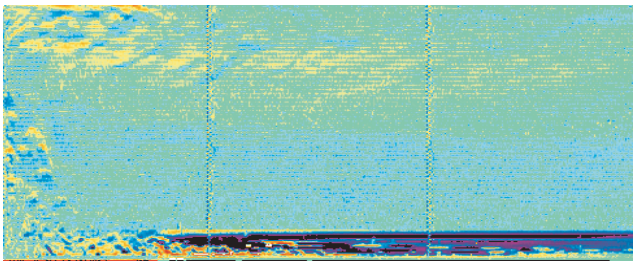

Figure 3. A synthetic schlieren image showing convection with thermal forcing alone. Image shows the full depth of the tank and 590mm of the 1.2m tank from the left end wall above the heated portion of the base. The two vertical lines are at 200mm intervals. Vertical scale is enlarged. Colour scale shows vertical refractive index gradient (red-yellow unstable; blue-black stable). Turbulent convection is seen at the left end; the interior has neutral (green) density gradient; and convection from the base erodes the stable bottom boundary layer flowing from the right.

Results with a salinity buoyancy flux

A range of experiments was carried out with different salinity fluxes by changing Q and ΔS. At the smallest salt fluxes ($B_S/B_T = 0.40$, $R_\rho = 1.4\text{x}10^{-5}$) the salt solution formed a thin layer that covered only about 100mm of the heated base before reaching a maximum length. The length of the layer at any time appeared to be governed by a balance between buoyancy (of the salty layer), inertia (of the oncoming flow) and viscous stress at the interface above. The salty layer reached a maximum extent when the flux of salt across the interface became larger than the source flux, causing the local density ratio across the interface to decrease. The layer later overturned into the overlying basin-scale circulation. It is expected that the salt flux slightly decreased the buoyancy available to drive the upwelling and temporarily weakened the overall circulation. The cycle repeated.

At large salt fluxes ($B_S/B_T = 1.4$) the salt solution formed a bottom layer that spread over much the heated base, and then lifted off the base to form an intrusion above the cold boundary layer. Salt fingering was visible beneath the intrusion, which eventually extended to the far end of the box and established recirculation in a bottom, salty layer. Convection confined to this layer then carried most of the heat flux through the box. Heat transfer through the top of the bottom layer formed a sharp double-diffusive interface of the 'diffusive' type and a much weaker large-scale circulation was visible in the overlying water, isolated from the base.

At intermediate salt fluxes the flow underwent several oscillations, corresponding to formation and breakdown of a warm, salty layer at the heated end. The oscillatory behaviour was confirmed in temperature records such as those in figure 4. The first few breakdowns fed salty water into the upwelling plume, which carried it to the top, and convection persisted through the full depth of the box. Growth of each salty layer caused a cooling (thickening) of the boundary layer elsewhere. However, subsequent breakdowns of the salty layer gave rise to an intrusion of salty water along the top of the cold boundary layer, and this propagated the full length of the box. Salt fingering was visible between this intrusion and the underlying fresher boundary layer. The cycle repeated but after several breakdowns the convection became isolated to a shallow bottom layer of relatively warm, salty water (about 50 - 70mm deep) and convection in the remainder of the water column was then driven only by the heat flux through a diffusive interface.

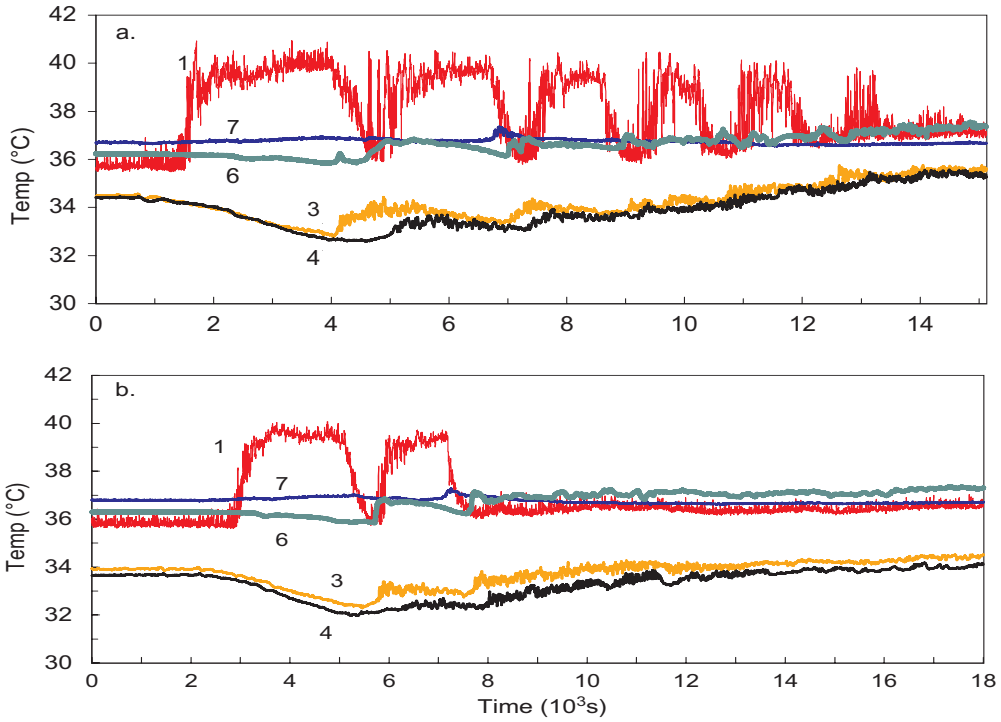

Figure 4. Temperature records from runs with a) ΔS = 0.51%, Q = 3.6x10^{-7}m^{3}s^{-1}, B_S/B_T = 1.04 and b) ΔS = 0.45%, Q = 4.2x10^{-7}m^{3}s^{-1}, B_S/B_T = 1.15. Records shown are from thermistors #1, 3 and 4 in the bottom boundary layer, #6 immediately above the boundary layer and #7 near the top of the box (figure 1). Salt fluxes began at a) 600s and b) 2040s. Record #1 shows that the density interface at the top of the salty layer passed across the thermistor as the layer grew and broke down. The salt layer growth thickened the cold boundary layer at the other end of the box. The first two breakdowns introduced greater fluxes of heat and salt to the top of the box (thermistor #7), but there were stronger warming events at thermistors # 3, 4 and 6.

Conclusions

The conceptually simple problem of convection in a channel, forced by a lateral gradient of temperature or heat flux at its base and a stabilising salinity flux at one end, can serve as a useful model with which to explore fundamental aspects of convection dynamics that may be relevant to the oceanic thermohaline circulation. In particular, the experiment is designed to model the effects of a stabilising surface freshwater buoyancy flux into the ocean at high latitudes. Inverting the model and interpreting it in oceanic terms we find a stable 'subtropical thermocline' near the surface and a convectively mixed surface layer that deepens towards the 'polar' end of the basin. The salinity buoyancy flux tends to increase locally the stability of the surface mixed layer and leads to a 'high latitude' halocline. Deep convection continues to occur in a tightly confined region.

The addition of a sufficiently large salinity buoyancy flux can lead to strong stabilisation of the surface layer and isolation of much of the water column from the forcing boundary. This corresponds to a flooding of the upper ocean with relatively fresh waters and a switching off of the deep convection. The oscillatory behaviour seen under a range of (steady) salt fluxes involves fluctuations of the depth of penetration of the deep convection and of 'poleward' transport in the surface layer. Our goal has been to obtain insights into these complex processes and to develop useful parameterisations of the conditions under which the different circulation regimes occur. Future work will address the time scales of the response, the effects of variations in imposed heat and salt fluxes, and Coriolis effects.

Acknowledgments

We thank Tony Beasley and Chris Morgan for construction of the convection tanks and laboratory assistance.

References

[1] Bard, E., Hamelin, B., Arnold, M, et al., Deglacial sea-level record from Tahiti corals and the timing of global meltwater discharge, *Nature*, **382**, 1996, 241-244.

[2] Broecker, W. S., Peng, T.-H., Jouzel, J. & Russell, G., The magnitude of global fresh-water transports of importance for ocean circulation, *Climate Dyn*., **4**, 1990, 73-79.

[3] Dalziel, S. B., Hughes, G. O. & Sutherland, B. R., Whole-field density measurements by 'synthetic schlieren', *Experim. Fluids*, **28**, 2000, 322-335.

[4] Lenderink, G. & Haarsma, R. J., Variability and mutliple equilibria of the thermohaline circulation, associated with deep water formation, *J. Phys. Oceanogr*., **24**, 1994, 1480-1493.

[5] Manabe, S., & Stouffer, R. J., Simulation of abrupt climate change induced by freshwater input to the North Atlantic Ocean, *Nature*, **378**, 1995, 165-167.

[6] Rahmstorf, S., On the freshwater forcing and transport of the Atlantic thermohaline circulation, *Climate Dyn*., **12**, 1996, 799-811.

[7] Rossby, H.T., On thermal convection driven by non-uniform heating from below: an experimental study, *Deep-Sea Res*., **12A**, 1965, 9-16.

[8] Rossby, H. T., Numerical experiments with a fluid heated non-uniformly from below, *Tellus.*, **50A**, 1998, 242-257.

[9] Ruddick, B.R. & Schirtcliffe, T. G. L., Data for double diffusers: Physical properties of aqueous salt-sugar solutions, *Deep-Sea Res*., **26A**, 1979, 775-787.

[10] Thual, O. & McWilliams, J.C., The catastrophe structure of thermohaline convection in a two-dimensional fluid model and a comparison with low-order box models, *Geophys. Astrophys. Fluid Dyn*., **64**, 1992, 67-95.

[11] Stommel, H., On the smallness of the sinking regions in the ocean, *Proc. nat. Acad. Sci., Wash*., **48**, 1962, 766-772.

[12] Wadley, M. R., Bigg, G. R., Stevens, D. P., Johnson, J. A., Sensitivity of the North Atlantic to surface forcing in an ocean general circulation model. *J. Phys. Oceanogr*., **26**, 1996, 1129-1141.

[13] Winton, M. & Sarachik, E., Thermohaline oscillations induced by strong steady salinity forcing of ocean general circulation models, *J. Phys. Oceanogr*., **23**, 1993, 1389-1410.